Study of oxidized Cu(1 1 0) surface using noncontact atomic force microscopy

Shohei Kishimoto, Masami Kageshima *, Yoshitaka Naitoh, Yan Jun Li, Yasuhiro Sugawara

Department of Applied Physics, Osaka University, 2-1 Yamada-oka, Suita, Osaka 565-0871, Japan

A R T I C L E   I N F O

A B S T R A C T

Formation of an oxidized overlayer onto Cu(1 1 0) surface was examined by means of noncontact atomic force microscopy at oxidation temperature ranging from RT to 610 °C and an O_2 exposure from 10^4 to 10^5 L. Atomic resolution images of an c(6 × 2) reconstruction exhibited different contrasts from those obtained in STM studies and coincided well with the presented structural model. The surface oxidized at RT in the present exposure range exhibited a rough morphology, and was observed to undergo a partial transition to the c(6 × 2) structure at 25,000 L. At an oxidation temperature of 360 °C an well-ordered c(6 × 2) reconstruction was observed to cover the entire terrace irrespective of the exposure amount. Characteristic point defect was also imaged on this surface in detail. At an oxidation temperature of 610 °C a (2 × 1) reconstruction was observed to coexist on the same terrace with c(6 × 2). Formation mechanism of this coexistence phase in this high temperature regime is discussed.

© 2008 Elsevier B.V. All rights reserved.

1. Introduction

Oxidation of metal surfaces has drawn intense attention throughout the history of surface science as the typical example of surface chemical reaction. It is one of the methods to readily provide a surface with different characteristics, and oxidized metal surfaces are relevant also in various applicational fields like electronics, catalysis, etc. As the interest has been more oriented toward the microscopic aspects of the process, the more emphasis has been placed on characterization by using real-space imaging techniques like scanning tunneling microscopy (STM) [1] or atomic force microscopy (AFM) [2]. These techniques also initiated novel quantum-mechanical experiments of manipulating individual atoms or molecules into artificial nanometer-scale structures and probing their electronic properties in situ [3,4]. It should be noted that metals provide an ideal substrate for this kind of scientific approaches because of its structure-free electronic properties. An atomically-flat metal substrate combined with an atomically thin nitride passivation layer can decouple electronic perturbation from the substrate as demonstrated recently [5]. Since molecular oxygen has higher reactivity than nitrogen does, oxidation may provide another option for passivation [6]. The present work is motivated by necessity of a new well-characterized oxide layer formed onto a metal substrate.

In the present study Cu was chosen as the substrate among various candidate metals since the procedure to prepare atomi-cally-flat bare surface is well-established. Although its oxidation rate is low, especially at a high oxygen coverage, this will insure a well-passivated and inert oxide layer. It should be also noted that CuO is an especially relevant material to accommodate various quantum-mechanical phenomenon like superconductivity or giant magnetoresistance. Among the major low-index surfaces of Cu, the (1 1 0) surface is reported to have an initial oxidation rate about 10 times higher than that of the (0 0 1) surface [7]. In addition, its high anisotropy draws a scientific attention especially in its interaction with foreign atoms, molecules, and clusters.

Fig. 1 shows the summary of previous reports on the reconstruction of Cu(1 1 0) surface oxidized at various temperatures and O_2 exposures, together with results of the present study. These are roughly classified into two regimes, formation of a reconstructed two-dimensional overlayer [8–19] and growth of three-dimensional bulk Cu_2O islands [7,20]. In the present study, we have focused onto the former regime. It was reported that the Cu(1 1 0) surface transforms into a (2 × 1) structure with an oxygen coverage of 1/2 with an exposure around 1 L (1 L = 1.33 × 10^{-4} Pa s) to molecular oxygen at RT [8]. As the exposure is increased the (2 × 1) structure remains [8–10] until it exhibits transient to a c(6 × 2) structure with an oxygen coverage of 2/3 at an exposure of the order of 10^3 L [11,12]. At an exposure of 10^4–10^5 L the surface is predominantly covered with the c(6 × 2) structure [11]. A similar transition from the (2 × 1) structure to the c(6 × 2) was reported at an oxidation temperature around 100 °C [12–14] and the latter structure was reported to reign to an exposure of 10^7 L [13]. Growth of the (2 × 1) structure has been studied also at elevated

* Corresponding author. Tel.: +81 6 6879 7854.
E-mail address: kage@ap.eng.osaka-u.ac.jp (M. Kageshima).
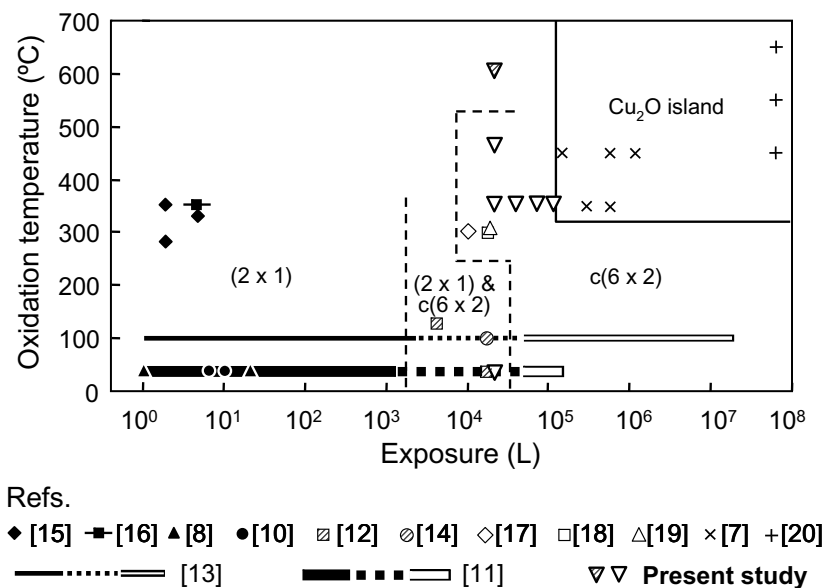
Fig. 1. Diagram of formation condition for various oxidized phases on Cu(110) surface. Results of the present study are also shown. The (2 × 1) structure is indicated with filled symbols or solid lines, the c(6 × 2) with open symbols or white lines, and the coexistence phase of the both with hatched symbols or dashed lines.

temperatures [15,16]. Remarkable reports were made that a well-ordered c(6 × 2) structure can be obtained at a substrate temperature of 300 °C and an exposure of the order of 10^4 L [17–19]. It was also reported that the critical exposure for the onset of transition from the (2 × 1) structure to the c(6 × 2) is lowered by raising the temperature from 27 °C to 127 °C [12]. Consequently interest arises whether a further increase in the oxidation temperature takes a positive effect on formation of c(6 × 2) overlayer or not. Therefore, in the present study, the experimental condition was mainly focused onto the temperature range higher than the reported condition, i.e., 360–610 °C and the exposure of 10^4–10^5 L. To check the consistency with the previous reports, oxidation at RT was also attempted.

Interest is also oriented to microscopic imaging of the atomic arrangement in the c(6 × 2) unit cell. Its detailed structural model was presented based on low energy ion scattering (LEIS) [21] and tensor low energy electron diffraction (TLEED) analyses [17]. On the other hand, in real space, STM images with atomic resolution reported by several research groups [12,14,18,19] are not completely consistent with each other, and thus identification of the observed features with the structural model is hardly possible. This is partly due to the nature of STM to image specific electronic states near the Fermi level rather than the atomic arrangement itself. It is known that noncontact (NC-) AFM [22] is capable of obtaining atomic resolution images and that its image contrast mainly arises from the chemical interaction force between the atoms on the tip apex and the sample surface [23]. Thus imaging with AFM is expected to provide more atomic or chemistry-oriented information on this surface and to complement real-space study of the c(6 × 2) structure. Also it should be mentioned that AFM study is preferable to STM for probing surfaces prepared under unprecedented condition which might induce structures or phases with an unexpectedly low conductance or a large band gap.

2. Experimental

The experiments were carried out in an ultra-high vacuum system equipped with a sample heater, an Ar ion gun, an oxygen inlet system and a home-built AFM apparatus [24] with an optical interference detection scheme. The base pressure of the system is better than 6×10^{-9} Pa. A single crystal Cu strip with a dimension of

2.5 mm × 10 mm × 0.5 mm, a purity of 99.999% and a miscut angle less than 0.4° was used as the substrate. The substrate initially covered with native oxide layer was cleaned by sputtering with Ar ion beam accelerated at 1 kV for 30 min and subsequently annealed at about 500 °C for 30 min. This cycle was repeated typically 15 times until a clean and flat surface was exposed. The heating was carried out via heat conduction from a Ta foil heater in contact with the sample via a boron nitride insulation sheet so that effect of direct current flowing in the sample is avoided. The temperature was monitored using an IR pyrometer (Konica-Minolta IR-308) with a detection wave length ranging 1.0–2.0 μm. Since the emissivity of Cu is typically 0.02 and is out of the settable range of this pyrometer, the measured temperature was corrected based on well-known Planck's law of radiation. Subsequent to the cleaning procedure, the sample was imaged with STM *in situ* by replacing the AFM cantilever with an etched W wire probe to confirm formation of an well-ordered clean Cu(110) surface. The oxidation was carried out in the preparation chamber by flowing high-purity O_2 gas into it while the sample was heated. During oxidation the chamber was evacuated with a turbo-molecular pump so that the pressure was kept at 1.3×10^{-3} Pa.

AFM imaging was carried out at RT in noncontact (NC) mode. A Si single crystal cantilever sensor with an integrated Si probe was employed in the measurement. Prior to the measurement, oxide layer and contamination on the probe surface was removed by sputtering with Ar ion, a procedure routinely used for obtaining an well-characterized bare Si probe. The typical resonance frequency and the spring constant of the cantilever were 150 kHz and 35 N/m, respectively. The cantilever was excited with positive feedback at its resonance frequency and its shift due to tip-sample interaction force was detected and was kept constant by regulating the tip-sample distance, while the oscillation amplitude was kept constant using an automatic gain control (AGC) system (a constant amplitude (CA) mode). For comparison with the previous reports, STM observation was also carried out.

3. Microscopic observation with high-resolution imaging of c(6 × 2) structure

The structural model for atomic arrangement in the c(6 × 2) unit cell was first proposed by Feidenhans'l et al. based on STM

and X-ray diffraction studies [14], and later determined more in detail in LEIS [21] and TLEED analyses [17]. Fig. 2 shows the atomic arrangement presented based on the TLEED result [17]. The model for the (2 × 1) reconstruction is also shown for comparison. The both structures are formed onto the layer of Cu atoms named "surface Cu" that retains arrangement of bulk structure except for a slight relaxation. A common feature for these two structures is rows of alternating Cu ("added Cu") and O atoms along the [001] direction adsorbed onto the "surface Cu" atoms. In the (2 × 1) phase the rows are arranged in every two atomic spacings along the [1$\bar{1}$0] direction to form the so-called "added-row" structure. On the other hand, in the c(6 × 2) structure, two Cu–O rows are paired with one atomic spacing, and each pair is connected with the neighboring ones with an additional topmost Cu atom ("super Cu") over a gap of two atomic spacings. The O atoms adjacent to this "super Cu" atom are elevated from the original level to form a characteristic unit of O–Cu–O along the [1$\bar{1}$0] direction forming a quasi-network structure of Cu and O atoms. This accounts for the two types of bonding configuration for the O atoms reported with electron energy loss spectroscopy (EELS) [25]. Hereafter, the elevated and the non-elevated O atoms are described as "high O" and "low O", respectively.

In the real-space study of atomic-scale structure, only STM has been employed and, to our knowledge, no report has been made using AFM. All of these STM images show one common feature; protrusions at each corner and the center of the unit cell [12,14,18,19]. Since their appearance showed weak dependence on the bias voltage or tunneling current, they were reasonably attributed to a spatially elevated site, i.e., the "super Cu" atom [14]. The rest of the observed features were, however, not always consistent with each other; some showed no contrast besides the "super Cu" [18,19], others complicated or unclear intra-cell contrast that could hardly be correlated to atomic arrangement [12,14]. This is probably due to the principle of the STM to detect specific electronic states around the Fermi level.

Under a standard imaging condition of NC-AFM, the attractive interaction between the probe and the sample is imaged. This means that a bright contrast in an atomically-resolved image is usually associated with sites that are topographically elevated or chemically reactive with the probe. If the former effect is domi-

nant, the "super Cu" site should appear as the brightest spot. On the other hand, the latter effect can impose different contrast and thus complicate the analysis. In the present study, since the probe apex was sputter-cleaned with Ar ion right before the AFM observation, the expected chemical species on the apex is Si. If once the probe is brought into interaction with the sample surface, however, species fluctuating or migrating on the surface may easily transfer to the apex. Therefore, it is not readily possible to specify the chemical species at the probe apex. Eventually the most practical experimental approach is to examine compatibility of each obtained image pattern with the proposed structural model.

The obtained image contrast in the unit cell of c(6 × 2) structure actually varied as is often the case with high-resolution imaging with scanning probe microscopy. Images obviously contrary to the surface symmetry were regarded as arising from asymmetric probe apex and were carefully excluded from analysis. Rest of the images can be classified into roughly three types, typical ones of which are shown in Fig. 3a–c, denoted as type-a, -b and -c, respectively. Although all these patterns were relatively stable compared to other inferior images reflecting tip asymmetry, switching of the image contrast between these patterns was sometimes observed even during imaging at relatively weak tip-sample interaction. This fact implies that the difference arose from the tip effect, not from the difference in the real atomic arrangement on the sample. It should be also noted that no phase shift in the image pattern was observed at such switching events, implying that the relative image registry in Fig. 3 is reasonable. The type-a image shows protrusions only at each corners and the center of the unit cell. This appearance seems to be consistent with the STM images in Refs. [18,19]. Actually this type of image was likely to be obtained in a situation where the probe tip had been slightly damaged by an accidental contact with the sample, and thus should be regarded as less-reliable. The fact that the "super Cu" site is imaged as an unexpectedly large protrusion also supports this inference. In contrast to this, the type-b shows an additional subsidiary contrast like a dim band running along [001] direction. This appearance is completely different from that in the STM images with subsidiary features in Refs. [12,14]. Although detail of these STM images are not completely consistent with each other, they show another common feature of a dim spot located between
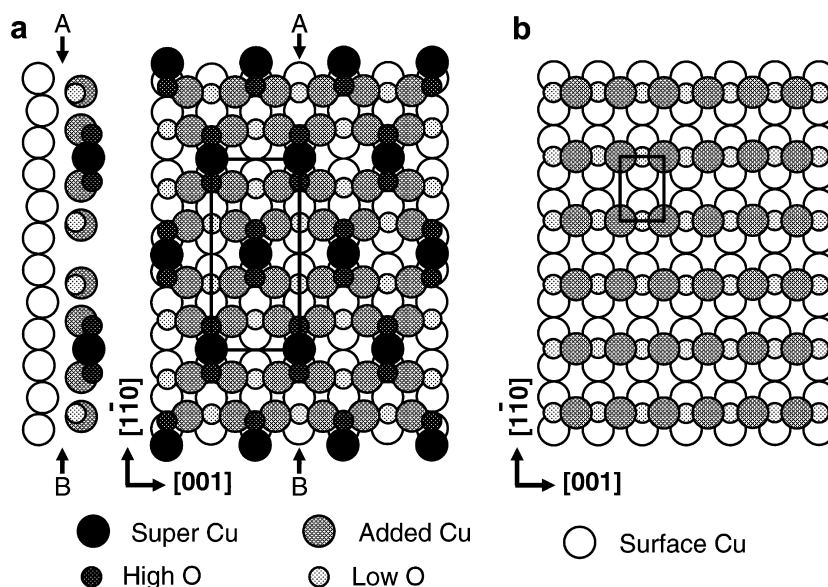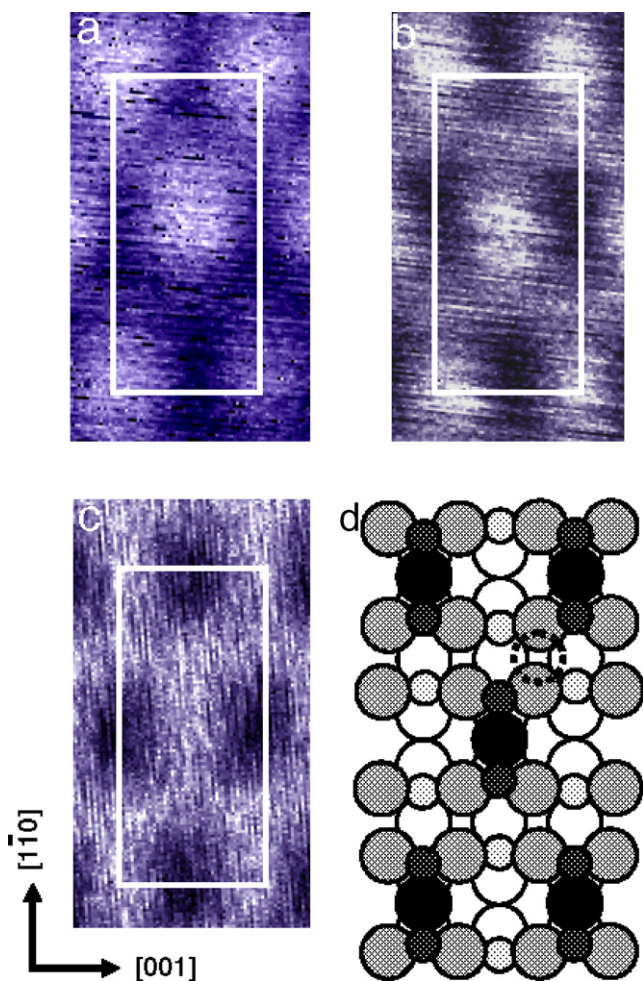

Fig. 2. (a) Illustration of atomic arrangement of the c(6 × 2) structure after Ref. [17] with a profile taken along line A–B, and (b) structure of the (2 × 1) reconstruction for comparison.

Fig. 3. (a–c) High-resolution AFM images of 12 Å × 21 Å area showing three types of contrast and (d) the corresponding atomic arrangement drawn assuming the structural model in Fig. 2a. The position of dim spot observed in STM images in Refs. [12,14] is indicated with a broken circle in (d).

two nearest "super Cu" sites. Appearance of these STM images cannot be explained from the topographical reason since this position corresponds to the midpoint between two "added Cu" atoms as indicated with a broken circle in Fig. 3d. On the other hand, in the type-b AFM image, the position and shape of the dim band match well with those of the assembly of "added Cu" and "low O" atoms. Also it should be noted that right after the initial approach of a fresh probe toward the surface the probability of obtaining this type of image was higher than the other two. Therefore, at the moment the type-b image should be regarded as the best-characterized one. Then the appearance of the type-c image is somewhat puzzling. In this image the bright spots are connected with each other, and consequently the contrast appears like a hexagonal network elongated along the $[1\bar{1}0]$ direction. Since this type of image has never been reported in any STM studies, it should be attributed to an effect specific to AFM. However, it cannot be explained by the discussion based on a simple topographic effect; probably modulation by chemical interaction must be taken into account. It is possible that the tip has picked up a species migrating on the surface. If the interaction between the new tip atom and the "high O" atom is enhanced, it can result in an appearance like this. The most possible tip atom is O, which should have many orbitals overlapped with those of the sample O atoms and thus have a strong attractive interaction with it. It is noteworthy that similar enhancement of chemical bonding force between a pair of like

atoms were previously reported [26]. To elucidate above hypothesis, further study with a better-characterized probe species is required.

## 4. Temperature and exposure dependence of c(6 × 2) reconstruction

Morphological feature of the surface covered with c(6 × 2) reconstruction was examined with oxidation temperature varied between RT and 610 °C. Fig. 4 shows the comparison of images obtained by RT oxidation with various exposure amounts ranging 10,000–25,000 L. In each case the surface exhibits a rough morphology with irregular protrusions and high-resolution imaging was not achieved stably due to accidental contact of the probe with the sample during scanning. At an exposure of 10,000 L the surface exhibited rough terraces outlined by steps with a typical height around one bulk monolayer spacing of 1.28 Å as shown in Fig. 4a. Although the shape of the steps are not straight, they tend to be aligned along the [0 0 1] direction. This is attributed to remaining one-dimensional character of the (2 × 1) added-row reconstruction, although the (2 × 1) periodicity was no longer observable. Instead, periodic arrangement of the c(6 × 2) reconstruction was sometimes barely observed in the depressed regions. At 20,000 L the surface exhibits further roughening, and elevated terraces now look like discrete irregular islands with 1–2 monolayer height as shown in Fig. 4b. These islands still tend to extend along the [0 0 1] direction. In Fig. 4c obtained at 25,000 L, it is shown that the irregular islands have decreased in net area. From this fact these islands are considered to consist of bare Cu or to contain insufficient amount of O atoms to form c(6 × 2) structure. Although the c(6 × 2) reconstruction is clearly resolved in depressed flat region in Fig. 4c, the islands still keep height of 1–2 monolayers. In lower right in Fig. 4c islands are observed to outline flat c(6 × 2) area depressed by one monolayer height from the surrounding terrace. If these islands mainly consist of Cu atoms as speculated above, these are considered to act as both sources and sinks for migrating Cu atoms and thus prevent growth of atomically-flat reconstruction region. For improvement of surface quality, it is required to enhance the migration of Cu atoms by raising the temperature so that the islands disappear by enhanced diffusion.

With an oxidation temperature of 360 °C the surface morphology exhibited striking improvement. Fig. 5 shows a series of images obtained with various exposure amount ranging from 20,000–120,000 L. Apart from details of local structures like steps, adsorbates etc., the surface exhibits consistent appearance dominated by well-ordered c(6 × 2) reconstruction and little dependence on the exposure amount is observed. Fig. 5a shows an adsorbate island pinning the step motion. It is remarkable that the upper terrace is outlined by three types of steps, namely along [0 0 1], $[1\bar{1}0]$, and $[3\bar{3}2]$ directions. The $[3\bar{3}2]$ direction is in the diagonal of the rectangular c(6 × 2) unit cell. Similar steps are imaged also in Fig. 5b and d. It should be noted that all of these $[3\bar{3}2]$ steps have height of 2–3 monolayers and have a vicinal descending slope towards the lower terrace. It is probable that these vicinal slopes play a crucial role in stabilizing the $[3\bar{3}2]$ step. These observations imply that the oxidation temperature of 360 °C is sufficient to drive the step morphology into its thermodynamical equilibrium.

In Fig. 5c, a defect site is also imaged as indicated with a white broken circle. For closer investigation, the area around this defect is magnified in Fig. 6. The most outstanding feature of this defect is a shift of a "super Cu" site toward $[\bar{1}10]$ direction. Based on the registry analysis by drawing a mesh of the c(6 × 2) periodicity as shown in Fig. 6, amount of this shift was estimated to be about
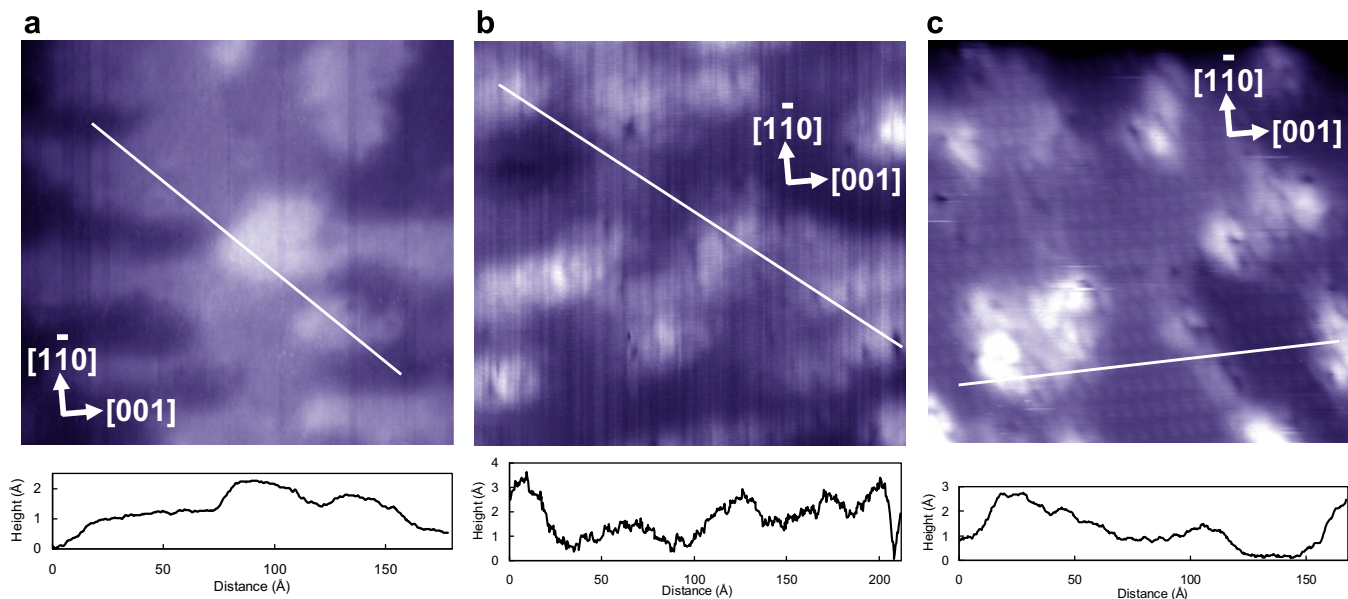
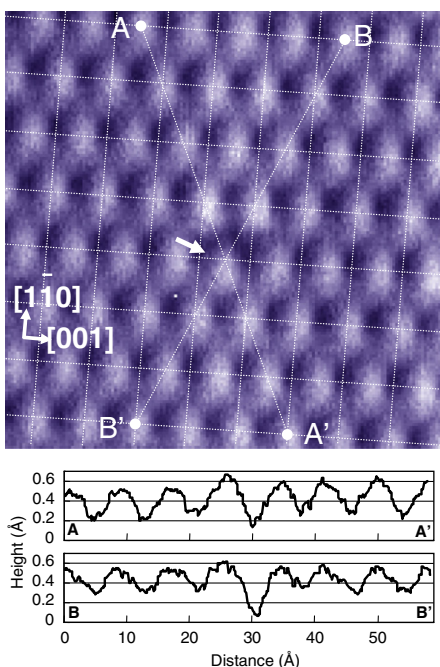**Fig. 4.** AFM images of 193 Å × 193 Å area of Cu(1 1 0) surface oxidized at RT with exposure amount of (a) 10,000 L, (b) 20,000 L and (c) 25,000 L. Profiles taken along the white lines in each image are also shown.
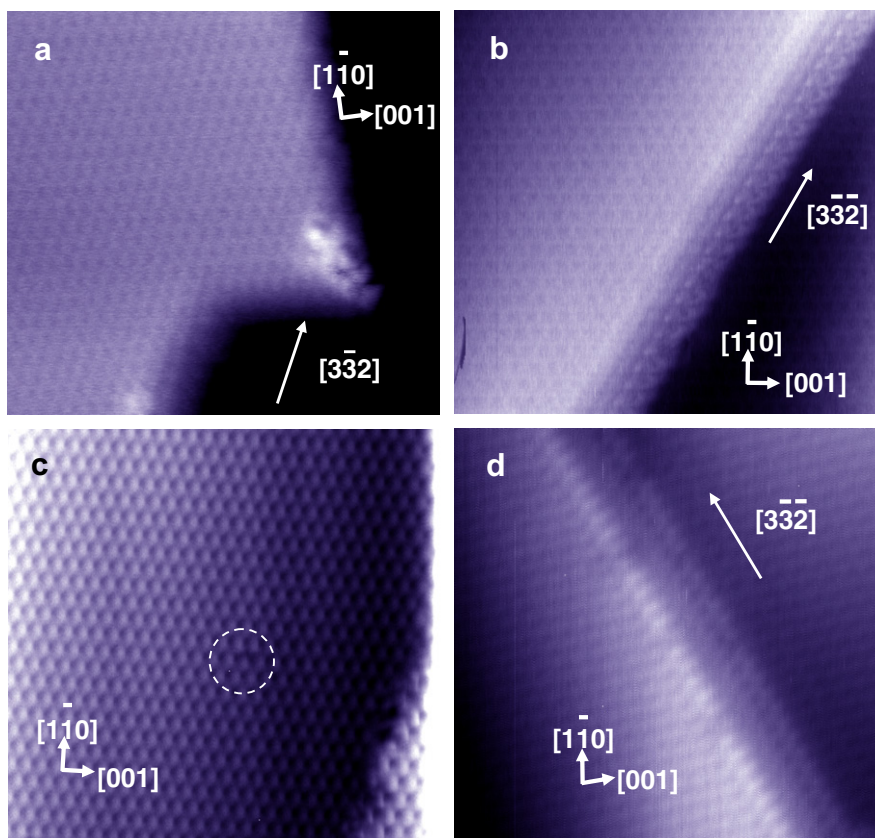
Fig. 5. AFM images of 185 Å × 185 Å area of Cu(1 1 0) surface oxidized at 360 °C with exposure amount of (a) 20,000 L, (b) 40,000 L, (c) 80,000 L and (d) 120,000 L.

1 Å. Since only this particular protrusion is shifted while the rest of equivalent sites are all unaffected, it cannot be attributed to any kind of measurement artifacts such as noise, thermal drift, feedback error, etc. In addition, since this appearance remained unchanged during several successive scanning over the same area, it should be attributed to a considerably stable structure. The

profiles taken along the two lines A–A′ and B–B′ are also shown in Fig. 6. These show that the two "super Cu" sites above the defect seem to be elevated by about 0.1 Å. It cannot be determined whether this elevation is really spatial one or is caused by modulation in the chemical reactivity with the probe. Although the hollows between these elevated sites and the shifted site are

Fig. 6. Magnified image of an area around the defect shown in Fig. 5c. A "super Cu" protrusion indicated with an white arrow is shifted toward $[\bar{1}10]$ direction by about 1 Å. Profiles along two lines along lines A–A′ and B–B′ are also shown.
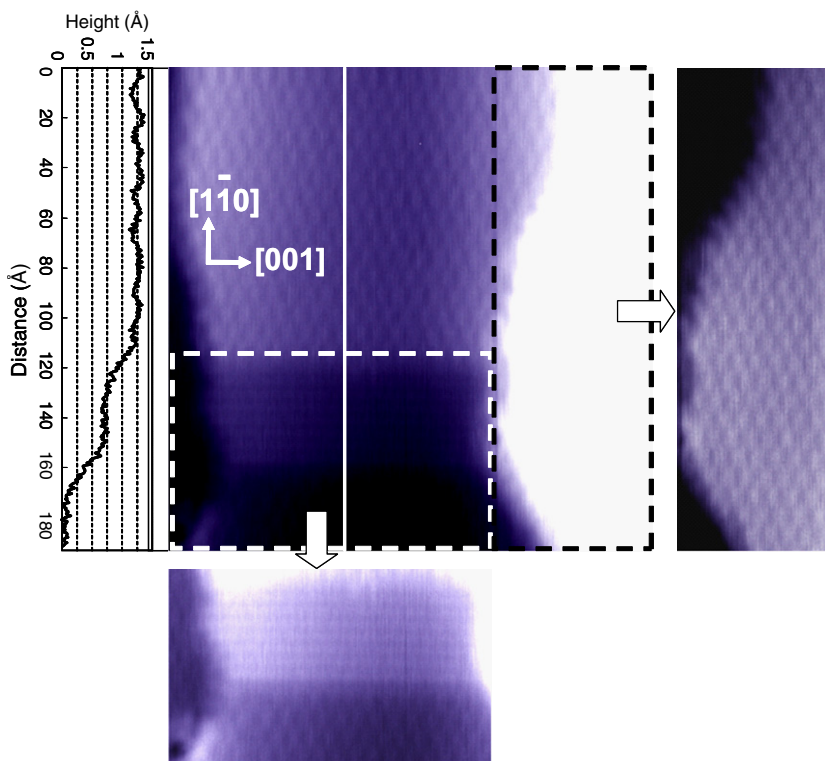
structure, such as an antisite of a segregated impurity atom. Missing atom is less probable; such a defective structure would be unstable at RT considering that even normal "super Cu" sites were reported to be mobile at RT [12,14].

It should be noted that the atomically-flat c(6 × 2) terraces prepared with the present condition were predominantly covered with well-ordered reconstruction, and the point defect described above was imaged only once in a series of several independent experimental runs. The maximum width of the single domain terrace observed in the present study was about 600 Å, which was limited by the spacing between the terraces due to miscut of the sample. Qualitatively same feature was observed also on a surface oxidized at 480 °C with exposure of 20,000 L.

At a higher oxidation temperature, however, a qualitative change was observed to take place. Fig. 7 shows an image of an area of 193 Å × 193 Å oxidized at 610 °C. Among four terraces shown in this image, the one on the right hand side is the highest and is completely covered with the c(6 × 2) reconstruction. Another terrace lower by one monolayer height is in upper center of the image. It is remarkable that the lower half of this terrace exhibits obviously different reconstruction. With the contrast adjusted as shown in Fig. 7, it exhibits a clear pattern of the 2 × 1 reconstruction. The line profile in Fig. 7 shows that the 2 × 1 region is lower than the c(6 × 2) one by about 0.5 Å as a consequence of lack in "super Cu" atoms. The profile also shows another lower terrace located at the bottom of the image, which is also covered with the c(6 × 2) structure as visualized by adjusting the contrast. Although another terrace at the left hand side of the image is too narrow to be imaged clearly, a faint mark of the c(6 × 2) reconstruction is barely visible.

In a large scale image shown in Fig. 8, a (2 × 1) region is imaged on a flat c(6 × 2) terrace as a depressed patch. Such (2 × 1) regions shared a common feature of quasi-rectangular shape elongated along the [001] direction. Their sides along the [001] direction

profiled much deeper than others, it might be simply that the probe could enter the hollow more deeply due to the enlarged spacing between these sites; it should not be straightforwardly attributed to a real structure. Since the effect of this defect structure is so localized, probably its origin is some atomic-scale

Fig. 7. AFM image of an 193 Å × 193 Å area of Cu(1 1 0) surface oxidized at 610 °C and 20,000 L. Partial images with offset gray-scale and a profile along the solid line are also shown.
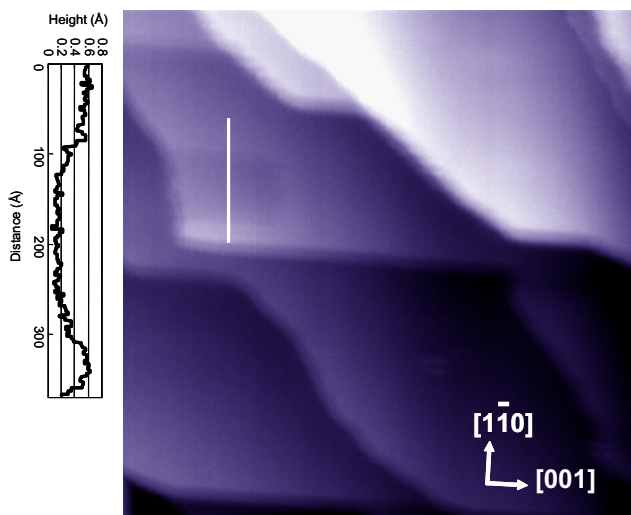
Fig. 8. AFM image of an 1600 Å × 1600 Å area of Cu(1 1 0) surface oxidized at 610 °C and 20,000 L. Images is slightly affected by multiple tip effect especially around the step edges. A patch-like region with the (2 × 1) reconstruction is imaged in the upper left. Profile taken along the solid line is also shown.
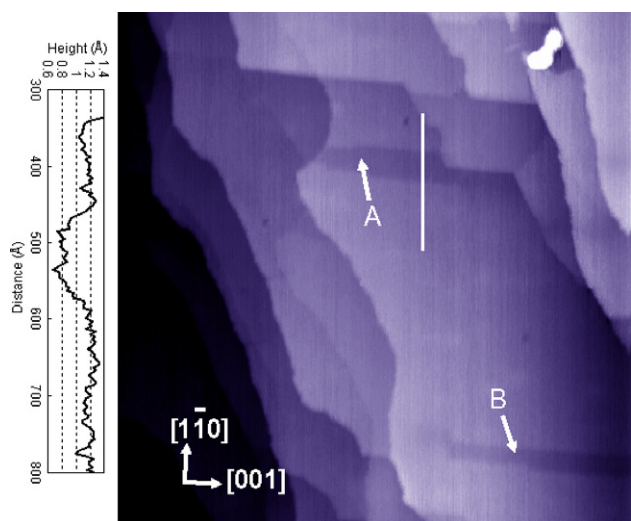
Fig. 9. STM image of a 1730 Å × 1730 Å area of the same surface as imaged in Figs. 7 and 8 obtained with a sample bias voltage of 0.1 V.

were fairly straight and longer than the ones in [1 $\bar{1}$ 0] direction in a ratio of often exceeding 5 to 1. While the (2 × 1) patch in Fig. 7 has both [0 0 1] and [1 $\bar{1}$ 0] steps on its sides, the one in Fig. 8 has only the [1 $\bar{1}$ 0] step.

Fig. 9 shows an STM image of the same surface taken for comparison with a sample bias voltage of 0.1 V. While the (2 × 1) patch "A" reaches to the [1 $\bar{1}$ 0] step, patch "B" is completely isolated from any steps. An STM study of a surface oxidized at 127 °C suggested preferential nucleation of c(6 × 2) structure at the step edges [12]. The present observation at the higher temperature seems to be somewhat contrary to this; the (2 × 1) patches can remain at step edges as well as in the middle of the terrace even after most of the terrace is covered with the c(6 × 2) structure. Interpretation of this observation will be discussed later.

The (2 × 1) patches in Fig. 9 are imaged as depression by about 0.4–0.5 Å from the surrounding c(6 × 2) area, showing little significant difference from AFM observation. This fact implies modulation in tunneling barrier height due to the difference in the

superstructure is less significant than topographic effect between these two regions, and thus supports the speculation that thickening of the insulating layer due to diffusion of O atoms into subsurface region had not taken place. Eventually formation of the (2 × 1) region is interpreted as simply due to decrease in the net amount of O atoms on the surface.

5. Discussion

The observation in the present study, especially the coexistence of the (2 × 1) and c(6 × 2), reveals some aspects of formation of the c(6 × 2) structure. Under the oxygen pressure and in the temperature range studied here, the transformation from the (2 × 1) to the c(6 × 2) is interpreted as a slow non-equilibrium path toward the free energy minima. It was reported that the c(6 × 2) structure is formed by exposure of as low as 1–10 L at a low temperature and subsequent annealing to 127–327 °C [27,28]. The striking difference in the critical O$_2$ exposure for formation of c(6 × 2) structure between the above two reports and the present study implies that the amount of metastable oxygen on the surface, whether as physisorbed molecules or dissociated atoms, plays a crucial role in formation of c(6 × 2). It was also reported that the c(6 × 2) structure annealed at a temperature above 387 °C transforms to the (2 × 1) [28]. Therefore, in 610 °C oxidation in the present study, formation of the c(6 × 2) region is presumed to have progressed in competition with the backward transformation from the c(6 × 2) structure to the (2 × 1). We consider this is the reason why coexistence of the c(6 × 2) and the (2 × 1) phases was observed in 610 °C oxidation. The apparent lack in preference for step edges of the (2 × 1) patches observed in Figs. 7–9 also can be explained as originating from the backward transformation to the (2 × 1) structure nucleated randomly on the terraces.

The oxidation conditions in the high temperature regime employed in the present study seem close to ones under which growth of bulk oxide island was reported [7,20], as shown in Fig. 1. In the present study, however, no mark of island nucleation was detected. We consider this is because the oxygen pressure in the above reports was of the order of 10^{-2}–10 Pa and was much higher than that in the present study. It was pointed out that the apparent activation barrier for island formation can be lowered by a thermodynamical effect under a high gas pressure [20] to promote formation of bulk oxide islands. Thus, the formation of bulk oxide islands should be of a different nature from that of (2 × 1) or c(6 × 2) structures observed in the present study.

6. Summary

Formation condition of an oxidized overlayer onto Cu(1 1 0) surface was searched through observation with NC-AFM. At an oxidation temperature of 360 °C and an exposure amount of 10^4–10^5 L, an well-ordered c(6 × 2) reconstruction was observed to cover the entire terrace. The image with atomic resolution exhibited a difference from STM images presented previously and coincided with the proposed structural model. A characteristic point defect was observed in detail and attributed to some stable atomic-scale singularity like antisite. At an oxidation temperature of 610 °C a (2 × 1) reconstruction with an oxygen coverage of 1/2 was observed to coexist on the same terrace with the c(6 × 2) structure. From the appearance of these (2 × 1) areas, the formation process of the c(6 × 2) phase in the high temperature regime is discussed

References

[1] G. Binning, H. Rohrer, Ch. Gerber, E. Weibel, Phys. Rev. Lett. 49 (1982) 57.
[2] G. Binning, C.F. Quate, Ch. Gerber, Phys. Rev. Lett. 56 (1986) 930.
[3] D.M. Eigler, E.K. Schweizer, Nature 344 (1990) 524.

[4] Y. Sugimoto, M. Abe, S. Hirayama, N. Oyabu, Ó. Custance, S. Morita, Nature Mater. 4 (2005) 156.
[5] C.F. Hirjibehedin, C.P. Lutz, A.J. Heinrich, Science 312 (2006) 1021.
[6] A.J. Heinrich, J.A. Gupta, C.P. Lutz, D.M. Eigler, Science 306 (2004) 466.
[7] G. Zhou, J.C. Yang, Surf. Sci. 531 (2003) 359.
[8] Y. Uehara, T. Matsumoto, S. Ushioda, Phys. Rev. B 66 (2002) 075413.
[9] F. Jensen, F. Besenbacher, E. Læsgaard, I. Stensgaard, Phys. Rev. B 41 (1990) 10233.
[10] D.J. Coulman, J. Wintterlin, R.J. Behm, G. Ertl, Phys. Rev. Lett. 64 (1990) 1761.
[11] G.R. Gruzalski, D.M. Zehner, J.F. Wendelken, Surf. Sci. 147 (1984) L623.
[12] D. Coulman, J. Wintterlin, J.V. Barth, G. Ertl, R.J. Behm, Surf. Sci. 240 (1990) 151.
[13] R. Feidenhans'l, I. Stensgaard, Surf. Sci. 133 (1983) 453.
[14] R. Feidenhans'l, F. Grey, M. Nielsen, F. Besenbacher, F. Jensen, E. Lægsgaard, I. Stensgaard, K.W. Jacobsen, J.K. Nørskov, R.L. Johnson, Phys. Rev. Lett. 65 (1990) 2027.
[15] K. Kern, H. Niehus, A. Schatz, P. Zeppenfeld, J. George, G. Comsa, Phys. Rev. Lett. 67 (1991) 855.
[16] R. Otero, Y. Naitoh, F. Rosei, P. Jiang, P. Thostrup, A. Gourdon, E. Lægsgaard, I. Stensgaard, C. Joachim, F. Besenbacher, Angew. Chem. Int. Ed. 43 (2004) 2092.

[17] W. Liu, K.C. Wong, K.A.R. Mitchell, Surf. Sci. 339 (1995) 151.
[18] P. Stone, S. Poulston, R.A. Bennett, N.J. Price, M. Bowker, Surf. Sci. 418 (1998) 71.
[19] M. Bowker, S. Poulston, R.A. Bennett, P. Stone, A.H. Jones, S. Haq, P. Hollins, J. Mol. Catal. A: Chem. 131 (1998) 185.
[20] G. Zhou, J.C. Yang, Appl. Surf. Sci. 222 (2004) 357.
[21] G. Dorenbos, M. Breeman, D.O. Boerma, Phys. Rev. B 47 (1993) 1580.
[22] F.J. Giessibl, Science 267 (1995) 68.
[23] T. Uchihashi, Y. Sugawara, T. Tsukamoto, M. Ohta, S. Morita, Phys. Rev. B 56 (1997) 9834.
[24] H. Ueyama, M. Ohta, Y. Sugawara, S. Morita, Jpn. J. Appl. Phys. 34 (1995) L1086.
[25] J.M. Mundenar, A.P. Baddorf, E.W. Plummer, L.G. Sneddon, R.A. Dino, D.M. Zehner, Surf. Sci. 188 (1987) 15.
[26] K. Yokoyama, T. Ochi, Y. Sugawara, S. Morita, Phys. Rev. Lett. 83 (1999) 5023.
[27] G.R. Gruzalski, D.M. Zehner, J.F. Wendelken, R.S. Hathcock, Surf. Sci. 151 (1985) 430.
[28] L.D. Sun, M. Hohage, P. Zeppenfeld, Phys. Rev. B 69 (2004) 045407.